PNAS RESEARCH ARTICLE | NEUROSCIENCE

SHP2 regulates GluA2 tyrosine phosphorylation required for AMPA receptor endocytosis and mGluR-LTD

Sanghyeon Lee[a,b,c,1], Jungho Kim[a,b,c,1], Hyun-Hee Ryu[a,b,d,1], Hanbyul Jang[a,b,d], DoEun Lee[a,b,c], Seungha Lee[a,b,c], Jae-man Song[a,b,c], Yong-Seok Lee[a,b,d,2], and Young Ho Suh[a,b,c,2]

Edited by Michisuke Yuzaki, Keio Gijuku Daigaku Igakubu Daigakuin Igaku Kenkyuka, Shinjuku, Japan; received October 2, 2023; accepted March 29, 2024 by Editorial Board Member Jeremy Nathans

Posttranslational modifications regulate the properties and abundance of synaptic α-amino-3-hydroxy-5-methyl-4-isoxazolepropionic acid (AMPA) receptors that mediate fast excitatory synaptic transmission and synaptic plasticity in the central nervous system. During long-term depression (LTD), protein tyrosine phosphatases (PTPs) dephosphorylate tyrosine residues in the C-terminal tail of AMPA receptor GluA2 subunit, which is essential for GluA2 endocytosis and group I metabotropic glutamate receptor (mGluR)-dependent LTD. However, as a selective downstream effector of mGluRs, the mGluR-dependent PTP responsible for GluA2 tyrosine dephosphorylation remains elusive at Schaffer collateral (SC)-CA1 synapses. In the present study, we find that mGluR5 stimulation activates Src homology 2 (SH2) domain-containing phosphatase 2 (SHP2) by increasing phospho-Y542 levels in SHP2. Under steady-state conditions, SHP2 plays a protective role in stabilizing phospho-Y869 of GluA2 by directly interacting with GluA2 phosphorylated at Y869, without affecting GluA2 phospho-Y876 levels. Upon mGluR5 stimulation, SHP2 dephosphorylates GluA2 at Y869 and Y876, resulting in GluA2 endocytosis and mGluR-LTD. Our results establish SHP2 as a downstream effector of mGluR5 and indicate a dual action of SHP2 in regulating GluA2 tyrosine phosphorylation and function. Given the implications of mGluR5 and SHP2 in synaptic pathophysiology, we propose SHP2 as a promising therapeutic target for neurodevelopmental and autism spectrum disorders.

SHP2 | mGluR5 | GluA2 | mGluR-LTD | trafficking

Significance

Glutamate receptors play an important role in learning, memory, and synaptic plasticity. Among them, group I metabotropic glutamate receptors (mGluRs) modulate the synaptic abundance of the GluA2 subunit of AMPA-type glutamate receptors, thereby contributing to synaptic long-term depression (LTD). Our study revealed that GluA2 tyrosine 869, along with the previously identified tyrosine 876, plays a pivotal role in mGluR-dependent LTD. Src homology 2 (SH2) domain-containing phosphatase 2 (SHP2), a nonreceptor protein phosphatase, protects and stabilizes GluA2 tyrosine 869 phosphorylation in its closed conformation. Upon mGluR5 stimulation, SHP2 transitions to the open conformation and dephosphorylates GluA2 tyrosine residues, leading to GluA2 internalization—a process underlying mGluR-LTD. This highlights the critical role of SHP2's conformational dynamics in maintaining synaptic function.

The strength of synaptic connections is readily altered bidirectionally in response to different stimuli. These synapse-specific modifications are forms of Hebbian-type synaptic plasticity, including long-term potentiation (LTP) and long-term depression (LTD), which are thought to be the cellular basis of learning and memory formation (1, 2). At the Schaffer collateral (SC)-CA1 synapses in the hippocampus, LTD can be triggered by the activation of either N-methyl-D-aspartate receptors (NMDAR-LTD) (3, 4), or group I metabotropic glutamate receptors (mGluR-LTD) (5, 6). Despite the two distinct mechanisms, LTD is eventually achieved by the removal of α-amino-3-hydroxy-5-methyl-4-isoxazolepropionic acid (AMPA) receptors from the postsynaptic membrane (1, 7–10).

The activity of Src-family protein tyrosine kinases (SFKs) is important for the regulation of AMPA receptor endocytosis (11, 12). Among the three tyrosine residues (3Y; Y869/Y873/Y876) at the extreme carboxyl terminus of GluA2 (GluA2ct), residue Y876 of the AMPA receptor GluA2 subunit has been extensively characterized as a target of SFKs, such as Src, Lyn, and Fyn (11, 13), as well as protein tyrosine phosphatases (PTPs) (12, 14, 15). Several studies have demonstrated that blocking PTP activity inhibits mGluR-LTD (16–20), which can be induced by paired-pulse low-frequency synaptic stimulation (PP-LFS) (21, 22) or by the application of a group I mGluR agonist such as (RS)- or (S)-3,5-dihydroxyphenylglycine (DHPG) (23, 24). The relevance of GluA2 tyrosine dephosphorylation in mGluR-LTD is further supported by the finding that the postsynaptic application of a short synthetic GluA2-3Y peptide (YKEGYNVYG) mimicking the tyrosine-rich region of GluA2ct disrupts GluA2 endocytosis and impairs mGluR-LTD (12, 25, 26). In particular, the GluA2 Y876 residue has been proposed as a potential target of PTP during mGluR-LTD (12, 14, 27).

Despite the importance of PTPs in regulating mGluR-LTD, the specific PTP that drives the tyrosine dephosphorylation of GluA2 remains largely unknown. Striatal-enriched protein phosphatase (STEP) has been identified as the PTP responsible for Y876 dephosphorylation in the hippocampus (15, 28). In addition, megakaryocyte protein tyrosine phosphatase (PTPMEG) has been suggested to be involved in GluD2-mediated cerebellar LTD (14). Interestingly, a recent study showed that GluA2 Y876F knock-in mice exhibit normal Hebbian plasticity, suggesting that GluA2 Y876 dephosphorylation may not be the sole mechanism underlying mGluR-LTD. However, phosphorylation of GluA2 Y876 is

The authors declare no competing interest.

This article is a PNAS Direct Submission. M.Y. is a guest editor invited by the Editorial Board.

[1]Sanghyeon Lee, J.K., and H.-H.R. contributed equally to this work.

[2]To whom correspondence may be addressed. Email: yongseok7@snu.ac.kr or suhyho@snu.ac.kr.

This article contains supporting information online at https://www.pnas.org/lookup/suppl/doi:10.1073/pnas.2316819121/-/DCSupplemental.

Published April 24, 2024.

necessary for homeostatic upscaling through the synaptic accumulation of glutamate receptor interacting protein 1 (GRIP1) (29).

Src homology 2 (SH2) domain-containing phosphatase 2 (SHP2) is a widely expressed nonreceptor PTP encoded by the *PTPN11* gene (30). SHP2 acts as a positive effector of several receptor tyrosine kinases (RTKs), promoting the activation of the small GTPase Ras and the mitogen-activated protein kinase (MAPK)/extracellular signal-regulated kinase (ERK) signaling pathway (31). SHP2 consists of two SH2 domains (N-SH2 and C-SH2), a PTP domain, and a C-terminal tail with two tyrosine residues (Y542 and Y580) that can be phosphorylated (30, 32). In its basal state, the catalytic activity of SHP2 is repressed by intramolecular interactions between the N-SH2 domain and the catalytic cleft of the PTP domain, forming a closed conformation. When the N-SH2 domain binds to tyrosine-phosphorylated RTKs or when SHP2 tyrosine residues are phosphorylated, SHP2 undergoes a closed-to-open conformational change. This exposes the catalytic cleft of SHP2, leading to activation of its full PTP activity (32, 33). Moreover, the activity of SHP2 can be modulated by shifting the balance between its three conformational states: closed inactive, partially open semiactive, and fully open active states (34). Notably, a recent study employing the SHP2 allosteric inhibitor 6-(4-amino-4-methyl-1-piperidinyl)-3-(2,3-dichlorophenyl)-2-pyrazinamine (SHP099) in conjunction with SHP2 mutations revealed that SHP2 can exert a phosphatase-independent action, that is, phosphosite protection of certain substrates from tyrosine dephosphorylation through a scaffolding effect by the SH2 domains (35, 36).

Accumulating evidence highlights the role of SHP2 in the regulation of glutamate receptor function and pathogenesis of neurodevelopmental disorders (37). Studies in SHP2 gain-of-function (GOF) mutant or SHP2-deficient mice have demonstrated that SHP2 plays an important role in learning, memory, and synaptic plasticity by regulating the phosphorylation and function of AMPA or NMDA receptors (38–46). Despite these findings, the precise molecular mechanisms by which SHP2 regulates AMPA receptor function and synaptic plasticity remain unclear.

In this study, we provide evidence that SHP2, as a downstream molecule of mGluR5, dynamically regulates tyrosine phosphorylation of GluA2 AMPA receptors in the hippocampus. Using two different types of SHP2 inhibitors and *Ptpn11*$^{Y542F/+}$ mice, we elucidated the role of SHP2 in GluA2 endocytosis and mGluR-LTD.

Results

mGluR5 Regulates SHP2 Phosphorylation at Y542. To determine whether stimulation of group I mGluRs affects SHP2 activation, we treated rat primary hippocampal neurons with the group I mGluR agonist DHPG. We found that DHPG increased tyrosine phosphorylation of SHP2 at Y542 by approximately twofold to threefold, but not at Y580 (Fig. 1 *A* and *B*), indicating SHP2 activation. Residue Y542 of SHP2 has been identified as a major phosphorylation site of SHP2 in vivo, and its phosphorylation is sufficient to activate the MAPK pathway by interacting with the N-SH2 domain and releasing the closed, inhibited PTP domain (47, 48). ERK in the MAPK pathway was also activated by DHPG treatment (Fig. 1 *A* and *B*). SHP1, a protein structurally related to SHP2, has phosphorylatable tyrosine residues (Y536 and Y564) analogous to the Y542 and Y580 residues of SHP2 (49). In contrast to SHP2, DHPG-stimulation did not phosphorylate SHP1 at either Y536 or Y564 (*SI Appendix*, Fig. S1), suggesting that DHPG selectively activates SHP2 by phosphorylating the Y542 residue.

To investigate which group I mGluR subtype is responsible for SHP2 activation, we treated primary hippocampal neurons with either a selective mGluR1 antagonist 7-(hydroxyimino) cyclopropa[b]chromen-1a-carboxylate ethyl ester (CPCCOEt) or a selective mGluR5 antagonist 2-methyl-6-(phenylethynyl)pyridine hydrochloride (MPEP). Interestingly, DHPG-induced Y542 phosphorylation of SHP2 was blocked by MPEP treatment, but not by CPCCOEt treatment (Fig. 1 *C* and *D*). Even with a high concentration of CPCCOEt (100 μM), which interfered with ERK phosphorylation, the level of SHP2 phospho-Y542 remained unchanged (*SI Appendix*, Fig. S2). Furthermore, the mGluR5 selective agonist (RS)-2-chloro-5-hydroxyphenylglycine (CHPG) increased the phosphorylation of SHP2 Y542 to a level comparable to that induced by DHPG (Fig. 1 *E* and *F*). When we knocked down (KD) mGluR5 using an shRNA lentivirus, no increase in SHP2 Y542 phosphorylation was observed in response to DHPG-stimulation (Fig. 1 *G* and *H*). Thus, our findings support the conclusion that mGluR5 activates SHP2 by phosphorylating Y542.

SHP2 Protects Steady-State GluA2 Phosphorylation at Y869 in Neurons. Based on our finding that SHP2 is activated upon mGluR5 stimulation, we investigated the role of SHP2 in regulating tyrosine phosphorylation of GluA2ct. We generated an shRNA lentivirus targeting SHP2, which effectively reduced SHP2 protein levels in primary hippocampal neurons while leaving SHP1 levels unaffected (Fig. 2*A*). We evaluated GluA2 tyrosine phosphorylation levels using two different GluA2 phospho-tyrosine antibodies. Unexpectedly, we observed a significant decrease in the signals detected with the anti-GluA2 p3Y antibody, whereas there was no notable change with the anti-GluA2 pY876 antibody (a gift from Kornau's lab) (12) (Fig. 2 *A* and *B*). The anti-GluA2 p3Y antibody recognizes GluA2, even if only one of Y869, Y873, or Y876 is phosphorylated. Given this discrepancy, we characterized the specificity of these GluA2 phospho-tyrosine antibodies. We conducted a dot blot analysis using synthetic phospho-peptides and found that the anti-GluA2 p3Y antibody preferentially recognized phosphorylated Y869, whereas the anti-GluA2 pY876 antibody exclusively recognized phosphorylated Y876 (*SI Appendix*, Fig. S3 *A* and *B*). We subsequently developed an antibody that specifically targeted GluA2 phosphorylated at Y869 by cross-adsorbing the anti-GluA2 p3Y antibody with a GluA2ct Y869F protein phosphorylated at both Y873 and Y876 (*SI Appendix*, Fig. S3 *A*, *B*, and *E*). The anti-pY869 antibody had minimal cross-reactivity with GluA3 pY874 analogous to GluA2 pY869, whereas Kornau's anti-pY876 antibody exhibited substantial cross-reactivity with GluA3 pY881 analogous to GluA2 pY876 (*SI Appendix*, Fig. S3 *C* and *D*). The specificity of the anti-GluA2 pY869 and anti-GluA2 pY876 antibodies was further validated using HEK 293 T cells expressing GluA2 nonphosphorylatable phenylalanine (Phe, F) mutants (*SI Appendix*, Fig. S3 *E* and *F*), and these antibodies were used throughout this study. Because we observed that GluA2 phospho-Y869 levels decreased rather than increased upon SHP2 depletion (Fig. 2 *A* and *B*), we hypothesized that SHP2 protects and stabilizes the phosphorylation of GluA2 Y869 by serving as a phosphatase-independent scaffold instead of acting as a conventional PTP.

To determine whether GluA2 Y869 phosphorylation is regulated by neuronal SFKs or PTPs, we treated primary hippocampal neurons with 4-amino-5-(4-chlorophenyl)-7-(dimethylethyl) pyrazolo[3,4-d]pyrimidine (PP2), an SFK-specific inhibitor, or sodium orthovanadate (Na_3VO_4), a pan-PTP inhibitor. Similar to Y876, a well-known target of SFKs and PTPs, phosphorylation at Y869 was eliminated by PP2 treatment and increased by Na_3VO_4

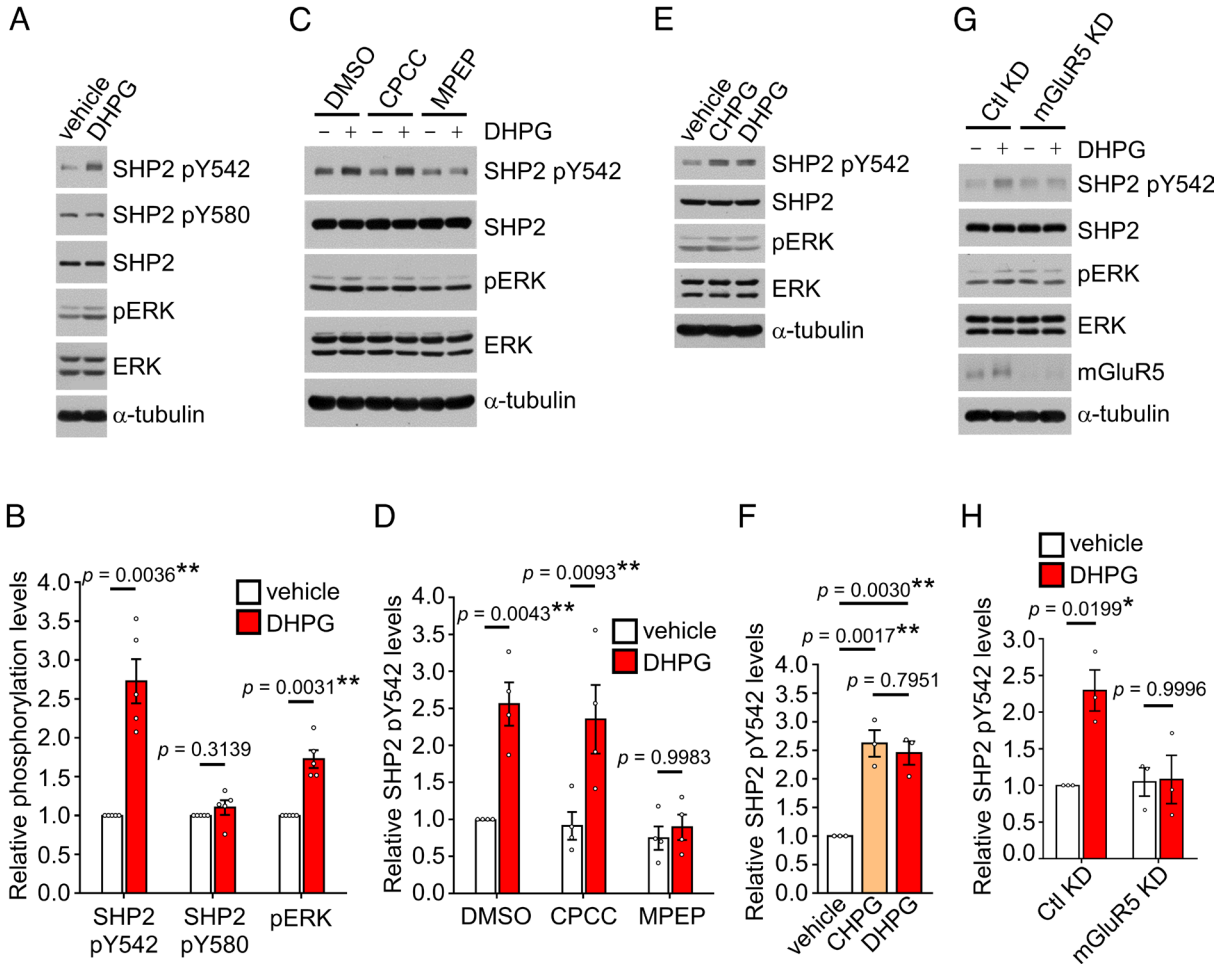

Fig. 1. mGluR5 stimulation activates SHP2 through phosphorylation at Y542. (*A*) Primary hippocampal neurons (DIV 14 to 16) were treated with 100 μM DHPG for 10 min. Representative western blots are shown. (*B*) Quantification data from panel (*A*) (n = 5, paired Student's *t* test). (*C*) Primary hippocampal neurons were treated with 20 μM CPCCOEt (CPCC) or 10 μM MPEP for 20 min, and 100 μM DHPG was added for an additional 10 min. (*D*) Quantification data from panel (*C*) (n = 4, one-way ANOVA with Tukey's multiple comparison test). (*E*) Primary hippocampal neurons were treated with 1 mM CHPG, a selective mGluR5 agonist, or 100 μM DHPG for 10 min. (*F*) Quantification data from panel (*E*) (n = 3; one-way ANOVA with Tukey's multiple comparison test). (*G*) Primary hippocampal neurons were infected with lentivirus expressing shRNA against mGluR5 (mGluR5 KD) or a nonrelated target (Ctl KD) and then treated with 100 μM DHPG for 10 min. (*H*) Quantification data from panel (*G*) (n = 3, one-way ANOVA with Tukey's multiple comparison test).

treatment, indicating that GluA2 Y869 is a substrate for both SFKs and PTPs in neurons (*SI Appendix*, Fig. S4).

To corroborate the protective role of SHP2 in tyrosine phosphorylation at Y869 of GluA2, we overexpressed either the full-length SHP2 (SHP2-FL) or a truncated SHP2 containing only the SH2 domain (SHP2-SH2) in neurons, under SHP2-depletion conditions. Because of its autoinhibited closed conformation, SHP2-FL was unable to restore the decrease in GluA2 phospho-Y869 levels induced by SHP2 KD, possibly behaving as a dominant negative form (Fig. 2*C*). However, when SHP2-SH2 was overexpressed, GluA2 phospho-Y869 levels markedly increased (Fig. 2*C*). These observations indicate that the SH2 domain, when released from its autoinhibited conformation, can effectively protect and stabilize Y869 phosphorylation in GluA2. This protective scaffolding function of the SH2 domain of SHP2 has been previously documented in the regulation of tyrosine phosphorylation of GAB1, GAB2, and SIRPα (36, 50).

To further delineate the function of SHP2 as a protective scaffold or a phosphatase, we used two distinct small-molecule inhibitors with different molecular mechanisms. The allosteric inhibitor SHP099 reversibly stabilizes SHP2 in a closed, catalytically inactive conformation by binding to the interface of the N-SH2, C-SH2, and PTP domains (35, 36), whereas 8-hydroxy-7-[(6-sulfo-2-naphthyl)azo]-5-quinolinesulfonic acid (NSC87877) inhibits the PTP activity of SHP2 by binding to its catalytic cleft (51). When primary hippocampal neurons were treated with SHP099, we observed a remarkable decrease in GluA2 phospho-Y869 levels, but no significant change in GluA2 phospho-Y876 levels (Fig. 2 *D* and *E*). In contrast, NSC87877 treatment had no effect on GluA2 phospho-Y869 or phospho-Y876 levels (Fig. 2 *D* and *E*). These findings are likely attributable to the loss of the protective effect due to the inflexible closed conformation induced by SHP099. Thus, SHP2 works on GluA2 Y869 but not on Y876, through a phosphatase-independent mechanism in the basal state. SHP2 phospho-Y542 and ERK phosphorylation levels were also reduced by SHP099 treatment, but not by NSC87877 treatment (Fig. 2 *D* and *E*).

Furthermore, neither NSC87877 nor SHP099 significantly affected the levels of phospho-Y416 in the activation loop of SFKs, nor the levels of phospho-Y527 or phospho-Y507 in the autoinhibitory loop of SFKs (52) (*SI Appendix*, Fig. S5). Thus, altered SFK activity may not cause the decrease in tyrosine phosphorylation of GluA2 at Y869 induced by SHP099. Additionally, we observed a significant reduction in SHP2 binding to GluA2 in primary hippocampal neurons by SHP099 treatment, but not by NSC87877 treatment, indicating that the closed and inflexible conformation of

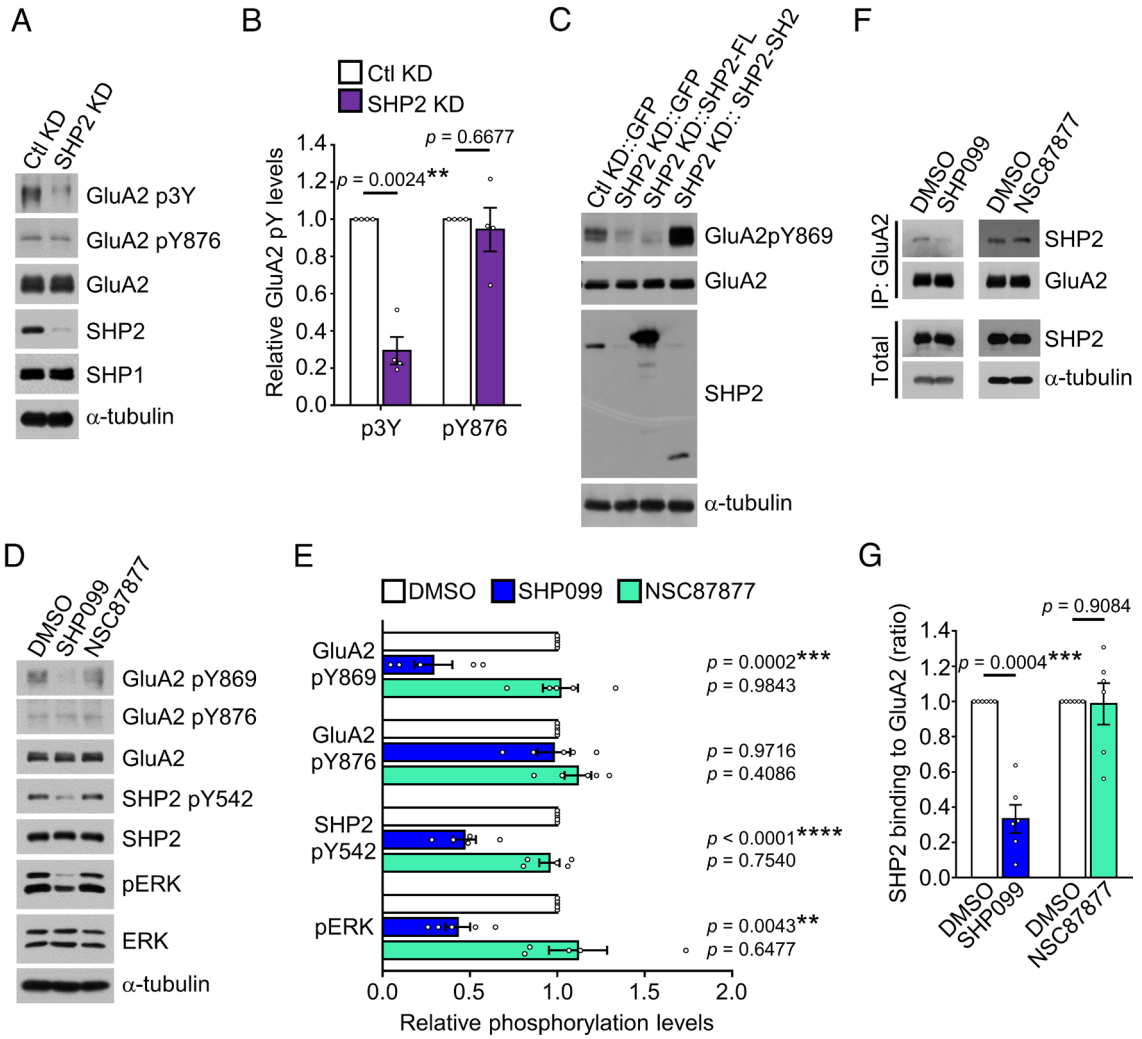

Fig. 2. SHP2 protects phospho-Y869 of GluA2 through its SH2 domain. (*A*) Primary hippocampal neurons were infected with lentivirus expressing either control shRNA (Ctl KD) or SHP2 shRNA (SHP2 KD) for 10 d. At DIV 14 to 16, western blot analysis was performed. (*B*) Quantification data from panel (*A*) (n = 4, paired Student's *t* test). (*C*) Primary hippocampal neurons were infected with lentivirus expressing either control shRNA (Ctl KD::GFP) or SHP2 shRNA (SHP2 KD::GFP), and simultaneously with SHP2 shRNA-resistant SHP2 full-length (SHP2 KD::SHP2-FL) or SHP2 SH2 domain fragment (SHP2 KD::SHP2-SH2) for 10 d. Representative western blots are shown. (*D*) Primary hippocampal neurons were treated with 10 μM SHP099 or 10 μM NSC87877 for 30 min and subjected to western blot assay. (*E*) Quantification data from panel (*D*) (n = 5, one-way ANOVA with Dunnett's multiple comparison test). (*F*) Binding analysis of SHP2 to GluA2. Inhibitor-treated neuron lysates were immunoprecipitated with an anti-GluA2 antibody, followed by immunoblotting with an anti-SHP2 antibody. (*G*) Quantification of relative SHP2 binding to GluA2 from panel (*F*) (n = 6, paired Student's *t* test).

SHP2 prevents its binding to GluA2 and thus cannot protect and stabilize GluA2 tyrosine phosphorylation (Fig. 2 *F* and *G*).

SHP2 Directly Binds GluA2 Phosphorylated at Y869. To investigate the role of GluA2 Y869 phosphorylation, we first determined whether GluA2 Y869 is phosphorylated by SFKs, using an in vitro kinase assay. When purified Glutathione-S-Transferase (GST)-GluA2ct (300 nM) was incubated with recombinant Src kinase (80 nM) for 30 min, we observed efficient phosphorylation of GluA2 Y869 and the well-known SFK substrate Y876 (11, 13) (*SI Appendix*, Fig. S6*A*). We also observed that both Fyn and Lyn kinases phosphorylated GluA2 Y869 and Y876 (*SI Appendix*, Fig. S6*B*). Next, using GST-GluA2ct harboring a single phosphorylatable site on either Y869 or Y876 (*SI Appendix*, Fig. S6*C*), we verified that Src could phosphorylate GluA2 at both Y869 and Y876 in vitro (*SI Appendix*, Fig. S6*C*). However, the phosphorylation level of Y876 in the GluA2 Y876 (Y869F/Y873F) mutant was lower than that observed in GluA2 WT, where both Y869 and Y876 are phosphorylatable. We further tested combinations of nonphosphorylatable mutants and found that when Y869 was nonphosphorylatable (Y876 or Y873/Y876), GluA2 Y876 was less efficiently phosphorylated by Src (*SI Appendix*, Fig. S6*D*). In addition, the affinity of the anti-pY876 antibody was not altered by the Y869 phosphorylation state (*SI Appendix*, Fig. S6*E*). These findings suggest that the phosphorylation of Y869 facilitates the phosphorylation of Y876, implying a permissive role for Y869 in Y876 phosphorylation.

We investigated whether SHP2 binds directly to GluA2ct, using a GST pull-down assay. First, recombinant Src kinase (80 nM) was used to phosphorylate GST-GluA2ct WT or the mutant lacking the 3Y domain (Δ865–883) (3 μM) for 2 h. To avoid inefficient phosphorylation resulting from the permissive effect, GST-GluA2ct was thoroughly phosphorylated by increasing the substrate concentration and extending the reaction time. We then incubated the phosphorylated GluA2ct (pGluA2ct) or non-pGluA2ct proteins with recombinant SHP2. Our results showed that SHP2 directly interacted with pGluA2ct WT, but not with pGluA2ct Δ865-883 or non-pGluA2ct WT (Fig. 3*A*). To identify the phosphorylatable residue of GluA2ct required critically for SHP2 binding, recombinant SHP2 was incubated with GST-pGluA2ct harboring nonphosphorylatable mutations. GST-pGluA2ct Y876F efficiently pulled down SHP2, whereas

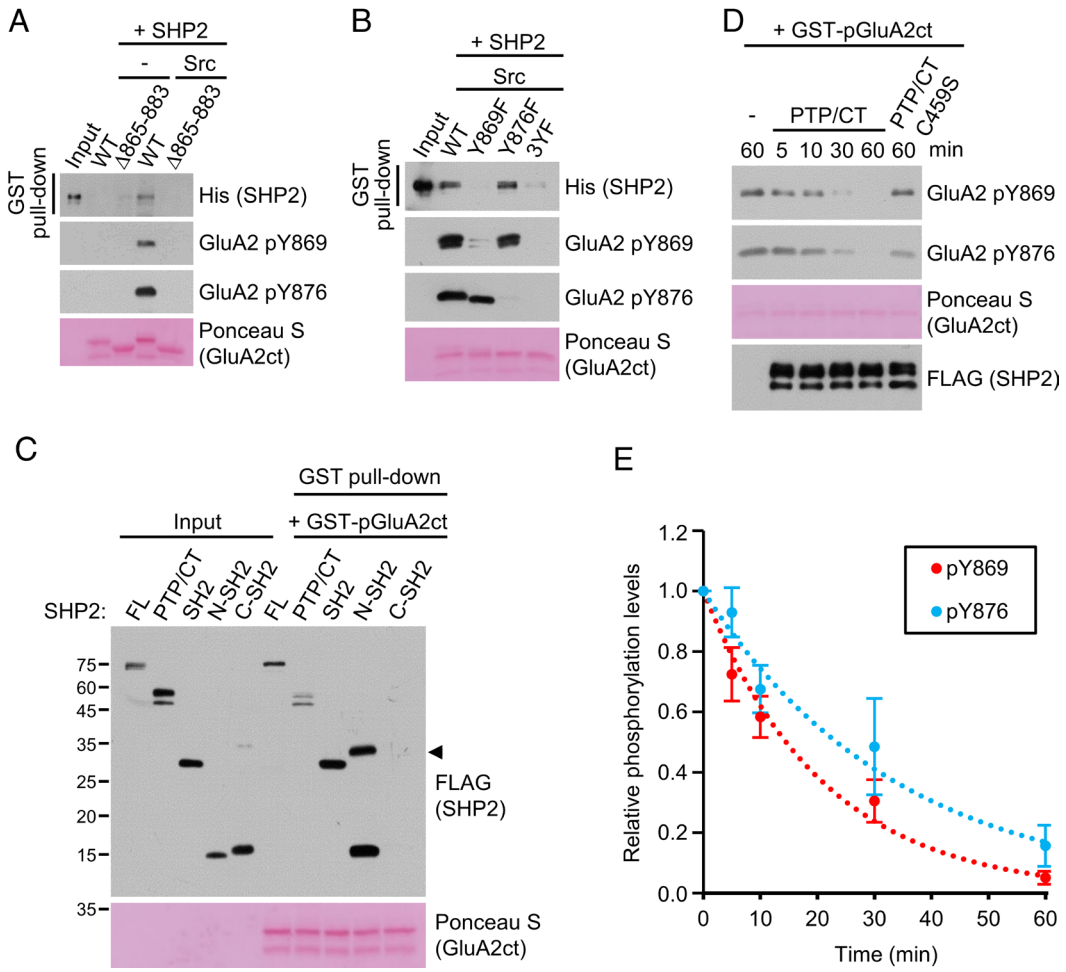

Fig. 3. SHP2 directly binds to GluA2 phosphorylated at Y869 and dephosphorylates GluA2 tyrosine residues. (*A*) GST pull-down assay to analyze direct binding between phosphorylated GluA2ct and recombinant SHP2. (*B*) Binding of recombinant SHP2 to pGluA2ct WT, Y869F, or Y876F. (*C*) The binding domain of SHP2 to pGluA2ct was analyzed using a GST pull-down assay. The arrowhead indicates the dimer of the N-SH2 fragment. (*D*) Recombinant SHP2 PTP/CT dephosphorylates GluA2 tyrosine residues. Src-phosphorylated GluA2ct was incubated with SHP2 PTP/CT. (*E*) Relative phosphorylation levels of each tyrosine residue from panel (*D*). The kinetics of SHP2-mediated dephosphorylation of GluA2 phospho-Y869 or phospho-Y876 was fitted using one-phase exponential decay curves (pY869, R^2 = 0.99, half-life = 14.4 min; pY876, R^2 = 0.98, half-life = 23.1 min; n = 4).

GST-pGluA2ct Y869F did not (Fig. 3*B*), indicating that the interaction between SHP2 and GluA2 depends on the phosphorylation state of Y869, but not that of Y876. To further analyze the domain of SHP2 binding to pGluA2ct, we incubated GST-pGluA2ct with recombinant SHP2 PTP/CT, SH2, N-SH2, or C-SH2 domains (*SI Appendix*, Fig. S7). We found that the SHP2 PTP, SH2, and N-SH2 domains interacted with pGluA2ct, whereas the C-SH2 domain did not (Fig. 3*C*). This observation indicates that GluA2 binds to both the N-SH2 and PTP domains of SHP2.

SHP2 PTP Dephosphorylates GluA2 Y869 and Y876 In Vitro. Since both Y869 and Y876 residues can be phosphorylated by Src and SHP2 can bind to GluA2ct, we next investigated whether SHP2 can directly exert phosphatase activity on tyrosine-phosphorylated GluA2ct. After phosphorylating GST-GluA2ct in vitro using Src, we incubated pGluA2ct with purified recombinant SHP2 PTP/CT protein lacking the SH2 domains. SHP2 PTP/CT does not form an autoinhibitory conformation, thus mimicking the open active form of SHP2 (*SI Appendix*, Fig. S7). We found that SHP2 PTP/CT effectively dephosphorylated GluA2 at both Y869 and Y876, whereas the catalytically inactive SHP2 PTP/CT C459S did not exhibit such activity (Fig. 3*D*). This observation indicates that both GluA2 Y869 and Y876 residues are direct substrates for SHP2 in vitro. Notably, SHP2 PTP activity exhibited faster dephosphorylation at GluA2 Y869 than at Y876 (Fig. 3*E*), suggesting that GluA2 Y869 is the preferred substrate for SHP2.

SHP2 Regulates DHPG-Induced GluA2 Tyrosine Dephosphorylation. Consistent with previous studies (12, 27), we observed that DHPG treatment reduced phosphorylation of GluA2 at Y876 in primary hippocampal neurons (Fig. 4 *A* and *B*). Surprisingly, we found that phosphorylation of GluA2 at Y869 was significantly reduced by DHPG treatment (Fig. 4 *A* and *B*). Of particular interest, treatment with NSC87877 blocked DHPG-induced dephosphorylation of both GluA2 phospho-Y869 and phospho-Y876 (Fig. 4 *A* and *B*). In contrast, when treated with SHP099, DHPG treatment did not result in a further decrease in GluA2 phospho-Y869 levels but reduced phospho-Y876 levels to the same extent as in the control (Fig. 4 *A* and *B*). These results suggest that DHPG-induced GluA2 Y869 dephosphorylation is regulated by the catalytic activity of SHP2 rather than by its protective function, as opposed to the basal state since the dephosphorylation was blocked by the catalytic activity-specific inhibitor NSC87877. In contrast, the disparate result for the phospho-Y876 suggests that DHPG-induced GluA2 Y876 dephosphorylation can be driven by both SHP2 and other PTPs depending on the molecular context. SHP099 treatment alone

did not change the phospho-Y876 level, implying that the protective function of SHP2 is negligible in the basal state. However, as DHPG treatment resulted in the reduction of the phospho-Y876 level in the presence of SHP099 but not NSC87877, SHP2 likely exerts a significant protective function against other PTPs as well as catalytic action in the DHPG-stimulated state. Considering that SHP2 can directly dephosphorylate both phospho-Y869 and phospho-Y876 in vitro (Fig. 3 *D* and *E*), it is reasonable to conclude that phospho-Y869 and phospho-Y876 are directly dephosphorylated by SHP2 upon mGluR stimulation.

To further validate the effect of SHP2 on GluA2 Y869 phosphorylation, we immunostained primary hippocampal neurons using an anti-GluA2 pY869 antibody. The specificity of the anti-GluA2 pY869 antibody in immunocytochemistry was confirmed in HEK 293 T cells cotransfected with Src and GluA2 Y869F, Y876F, or 3YF mutants (*SI Appendix*, Fig. S8*A*). Consistent with the western blot data (Fig. 4 *A* and *B*), we observed that NSC87877 prevented the DHPG-induced decrease in GluA2 Y869 levels, whereas SHP099 reduced both basal and DHPG-induced GluA2 Y869 levels (*SI Appendix*, Fig. S8 *B* and *C*).

SHP2 Controls Endocytosis of AMPA Receptors by Regulating GluA2 Tyrosine Phosphorylation Status. Based on the correlation between GluA2 tyrosine phosphorylation and the number of surface AMPA receptors (11, 15, 16, 25), we hypothesized that SHP2 plays a role in regulating surface AMPA receptor levels through the transduction of mGluR5 signals. To investigate the effect of SHP2 inhibitors on the expression of surface AMPA receptors, we used an antibody that recognizes the extracellular epitope of GluA2 to label the surface-expressed GluA2 in primary hippocampal neurons. DHPG treatment reduced surface levels of endogenous GluA2 (Fig. 4 *C* and *D*). Treatment with NSC87877 had little effect on steady-state surface GluA2 expression, but prevented the DHPG-induced decrease in surface GluA2 levels (Fig. 4 *C* and *D*). In contrast, treatment with SHP099 reduced surface GluA2 expression by approximately 60% under both basal and DHPG-stimulated conditions (Fig. 4 *C* and *D*). These changes in GluA2 surface expression closely correlated with alterations in GluA2 phospho-Y869 levels induced by SHP2 inhibitors under both basal and DHPG-stimulated conditions (Fig. 4 *C* and *D* and *SI Appendix*, Fig. S8 *B* and *C*).

We examined whether the tyrosine phosphorylation state affects the distribution of GluA2 at synapses by analyzing the synaptic versus extrasynaptic distribution of GluA2 phosphorylated at either the Y869 or Y876 residue. Interestingly, we found that GluA2 phosphorylated at Y869 was preferentially located in the Triton X-100 detergent-soluble extrasynaptic fraction, whereas GluA2 phosphorylated at the Y876 was more enriched in the detergent-insoluble PSD fraction (*SI Appendix*, Fig. S9).

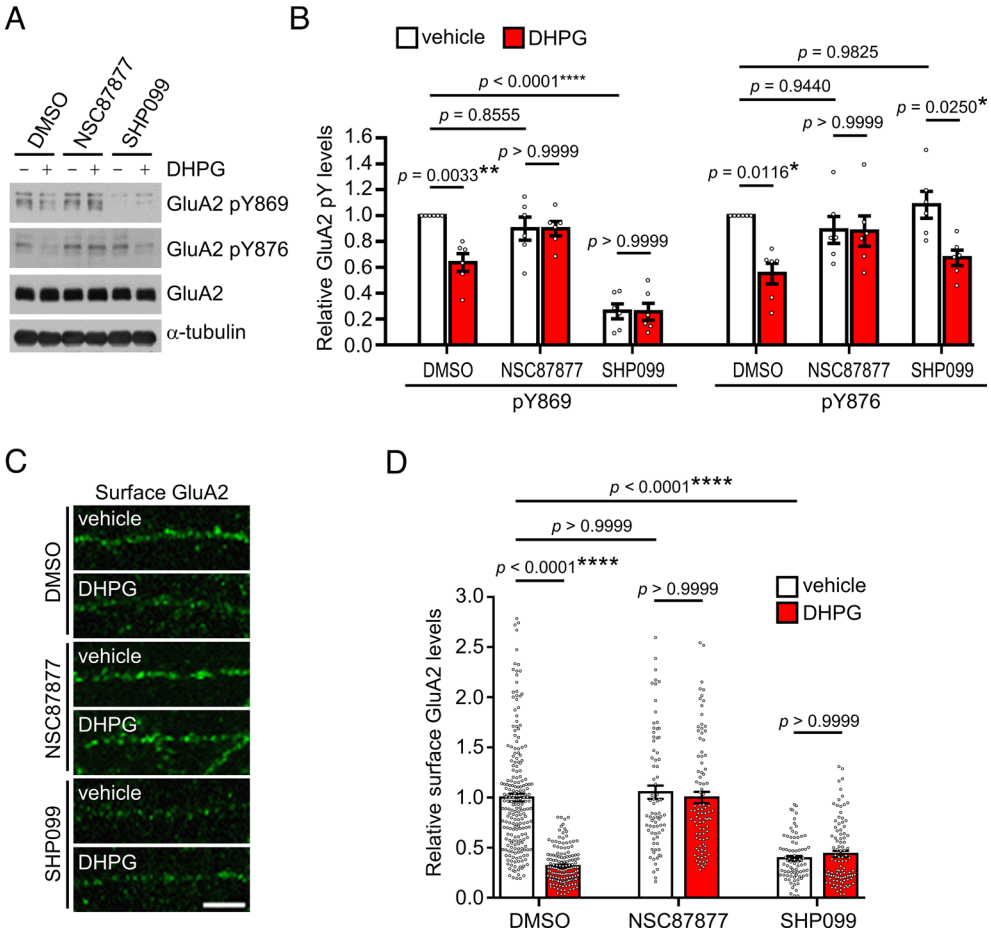

Fig. 4. SHP2 regulates GluA2 tyrosine phosphorylation and surface expression. (*A* and *B*) Effects of SHP2 inhibitors on the tyrosine phosphorylation levels of GluA2. (*A*) Primary hippocampal neurons (DIV 14 to 16) were treated with 10 μM NSC87877 or 10 μM SHP099 for 30 min, and 100 μM DHPG was added for an additional 10 min. Representative western blots are shown. (*B*) Quantification data from panel (*A*) (n = 6, one-way ANOVA with Tukey's multiple comparison test). (*C* and *D*) Effects of SHP2 inhibitors on the surface expression of GluA2. (*C*) Primary hippocampal neurons (DIV 14 to 16) were treated with 10 μM NSC87877 or 10 μM SHP099 for 30 min, and 100 μM DHPG was added for an additional 10 min. Neurons were subsequently incubated in conditioned medium for 15 min. For SHP099 experiments, SHP099 was added to the conditioned medium because of its reversible inhibitory properties. Surface-expressed GluA2 was immunostained under nonpermeabilized conditions. (Scale bar, 7 μm.) (*D*) Quantification of surface-expressed GluA2 from 30-μm-long secondary branches (n = 4, number of branches = 78–211, Kruskal–Wallis test with Dunn's multiple comparison test).

Next, we investigated the internalization rates of nonphosphorylatable GluA2 mutants under basal and DHPG-treated conditions. We expressed c-myc epitope-tagged GluA2 WT and nonphosphorylatable Y869F or Y876F mutants in primary hippocampal neurons and measured their internalization rates. Both GluA2 Y869F and Y876F mutants showed higher rates of internalization than WT GluA2 (*SI Appendix*, Fig. S10 *A* and *B*), indicating that dephosphorylation at either Y869 or Y876 is sufficient for GluA2 endocytosis. Further DHPG-induced internalization of the GluA2 Y869F or Y876F mutants was not observed, probably because of their enhanced steady-state endocytosis (*SI Appendix*, Fig. S10 *A* and *B*).

DHPG-Induced GluA2 Tyrosine Dephosphorylation and Endocytosis Are Impaired in *Ptpn11*$^{Y542F/+}$ Mice. To analyze the function of SHP2 downstream of mGluR5 under physiologically relevant conditions, we generated SHP2 Y542F knock-in mice (*Ptpn11*$^{Y542F/+}$) in which the SHP2 Y542 residue was replaced with a nonphosphorylatable Phe residue by standard homologous recombination (*SI Appendix*, Fig. S11 *A*–*C*). Except for one in 126 births, *Ptpn11*$^{Y542F/Y542F}$ homozygous mice were embryonically lethal, indicating an essential role of SHP2 Y542 phosphorylation in mouse survival (*SI Appendix*, Fig. S11*D*). Nissl staining of the entire brains of *Ptpn11*$^{Y542F/+}$ mice showed that the overall morphology was within the normal range (*SI Appendix*, Fig. S12 *A*–*D*). These results are consistent with those of a previous report showing no structural deficits in the brains of mice with forebrain-specific SHP2 deletion (38).

We evaluated the steady-state expression and phosphorylation levels of several synaptic proteins in *Ptpn11*$^{Y542F/+}$ mice. As expected, SHP2 phospho-Y542 levels were reduced by approximately 60% in the P2 fraction of the *Ptpn11*$^{Y542F/+}$ hippocampi. Compared to WT, no significant differences were observed in the levels of SHP2 phospho-Y580, GluA1, GluA1 phospho-S845, GluA2, GluN2B, GluN2B phospho-Y1252, GluN1, mGluR5, PSD-95, ERK, phospho-ERK, Src, Src phospho-Y416, and Src phospho-Y527 (Fig. 5*A*). However, we found that the phosphorylation level of GluA2 at Y869 was approximately 40% lower in *Ptpn11*$^{Y542F/+}$ mice, whereas phospho-Y876 levels were not significantly different (Fig. 5*A*).

To investigate the extent of the closed conformation adopted by SHP2 Y542F, we compared the catalytic activities of SHP2 WT and Y542F. Upon coexpression of GluA2 and Src, Y542F SHP2 reduced GluA2 phospho-Y869 and phospho-Y876 levels less effectively than WT SHP2 (*SI Appendix*, Fig. S13). This observation indicates that SHP2 Y542F adopts a more closed conformation than the WT SHP2.

We further investigated the changes in tyrosine phosphorylation of GluA2 upon DHPG treatment in cultured neurons from *Ptpn11*$^{Y542F/+}$ mice. DHPG treatment decreased GluA2 phospho-Y869 and phospho-Y876 levels in WT littermate neurons. However, the reduction in both residues was impaired in *Ptpn11*$^{Y542F/+}$ neurons, as DHPG treatment did not cause significant alteration in the phospho-Y869 and phospho-Y876 levels (n = 9, $P = 0.3743$ for pY869; n = 4, $P = 0.0776$ for pY876; Fig. 5 *B* and *C*). Moreover, the DHPG-induced increments in SHP2 phospho-Y542 and phospho-ERK levels were significantly reduced in *Ptpn11*$^{Y542F/+}$ neurons (Fig. 5 *B* and *C*). Thus, Y542F SHP2 lost its basal protective effect and impaired mGluR5-stimulated GluA2 tyrosine dephosphorylation at Y869 and Y876.

We observed a significant reduction in steady-state surface GluA2 levels and an impaired DHPG-induced decrease in surface GluA2 levels in the neurons of *Ptpn11*$^{Y542F/+}$ mice (Fig. 5 *D* and *E*). These indicate that SHP2 plays a crucial role in determining the endocytosis of GluA2 by controlling DHPG-induced dephosphorylation of GluA2 at Y869 and Y876.

SHP2 Inhibition Impairs mGluR-LTD. Our finding that SHP2 regulates mGluR-mediated AMPA receptor trafficking prompted us to examine the effect of SHP2 inhibition on mGluR-LTD. We recorded the extracellular field excitatory postsynaptic potential (fEPSP) at the hippocampal SC-CA1 synapses. We first induced mGluR-LTD either chemically with DHPG or synaptically by delivering PP-LFS, in the presence of NSC87877 or SHP099. We found that both DHPG-LTD and PP-LFS-LTD were impaired by NSC87877 (Fig. 6 *A* and *B* and *SI Appendix*, Fig. S14*A*), but not by SHP099 (Fig. 6 *C* and *D* and *SI Appendix*, Fig. S14*B*).

Next, we examined the electrophysiological characteristics of *Ptpn11*$^{Y542F/+}$ mice. When we compared mGluR-LTD in WT and *Ptpn11*$^{Y542F/+}$ mice, induced by either DHPG or PP-LFS, we found that although DHPG-induced LTD was normal (Fig. 6*E* and *SI Appendix*, Fig. S14*C*), PP-LFS-induced LTD was partially but significantly impaired (Fig. 6*F* and *SI Appendix*, Fig. S14*C*) in *Ptpn11*$^{Y542F/+}$ mice. In contrast, LFS-induced LTD was not significantly altered in *Ptpn11*$^{Y542F/+}$ mice (*SI Appendix*, Fig. S15), indicating that NMDAR-LTD is normal in *Ptpn11*$^{Y542F/+}$ mice. Additionally, we measured basal synaptic transmission by analyzing the input–output (I/O) relationship between the presynaptic fiber volley and fEPSP slopes and observed no significant difference in the I/O relationship between *Ptpn11*$^{Y542F/+}$ mice and WT littermates (*SI Appendix*, Fig. S16*A*). We also measured the paired-pulse ratio (PPR), which is defined as the ratio of the second fEPSP slope to the first fEPSP slope in response to paired-pulse stimulation. PPR showed a slightly higher, but statistically insignificant, trend in *Ptpn11*$^{Y542F/+}$ mice than in their WT littermates (*SI Appendix*, Fig. S16*B*), suggesting that the Y542F mutation does not affect presynaptic function.

Discussion

In the present study, we identified SHP2 as a downstream regulator of mGluR5 function. Under steady-state conditions, SHP2 interacts with GluA2 phosphorylated at Y869 and protects it from dephosphorylation, without exhibiting phosphatase activity. Upon mGluR5 stimulation, SHP2 is phosphorylated at Y542, inducing a conformational transition that enables SHP2 to exhibit phosphatase activity. SHP2 then dephosphorylates GluA2 at both Y869 and Y876, triggering GluA2 endocytosis and mGluR-LTD (*SI Appendix*, Fig. S17). Our findings reveal that SHP2 has a dual function related to GluA2. First, as a scaffold, it protects GluA2 tyrosine phosphorylation from dephosphorylation and maintains GluA2 on the surface. Second, it catalyzes the dephosphorylation of GluA2 tyrosine residues through its PTP activity, which is required for mGluR-LTD.

While GluA2 phosphorylated at Y869 and Y876 is found endogenously in the brain (53), previous studies on GluA2 AMPA receptor endocytosis and LTD have primarily focused on the GluA2 Y876 residue (12, 14, 27). In this study, however, we found a pivotal role of the GluA2 Y869 residue as a substrate for SHP2 in the modulation of AMPA receptor trafficking. Particularly, the surface expression of GluA2 was more closely associated with phospho-Y869 levels than with phospho-Y876 levels. The regulation of mGluR-LTD seems to involve two tyrosine residues on GluA2 rather than only one. Additionally, mGluR stimulation may activate multiple PTPs, including SHP2, leading to functional redundancy in the regulation of the GluA2 AMPA receptor subunit.

Importance of the GluA2 Y869 Residue As a Substrate for SHP2. We demonstrated that both the N-SH2 and PTP domains of SHP2 bind to phosphorylated GluA2 at Y869. Typically, when the N-SH2 domain interacts with conventional target substrates, it exposes the catalytic cleft of SHP2, resulting in an open conformation

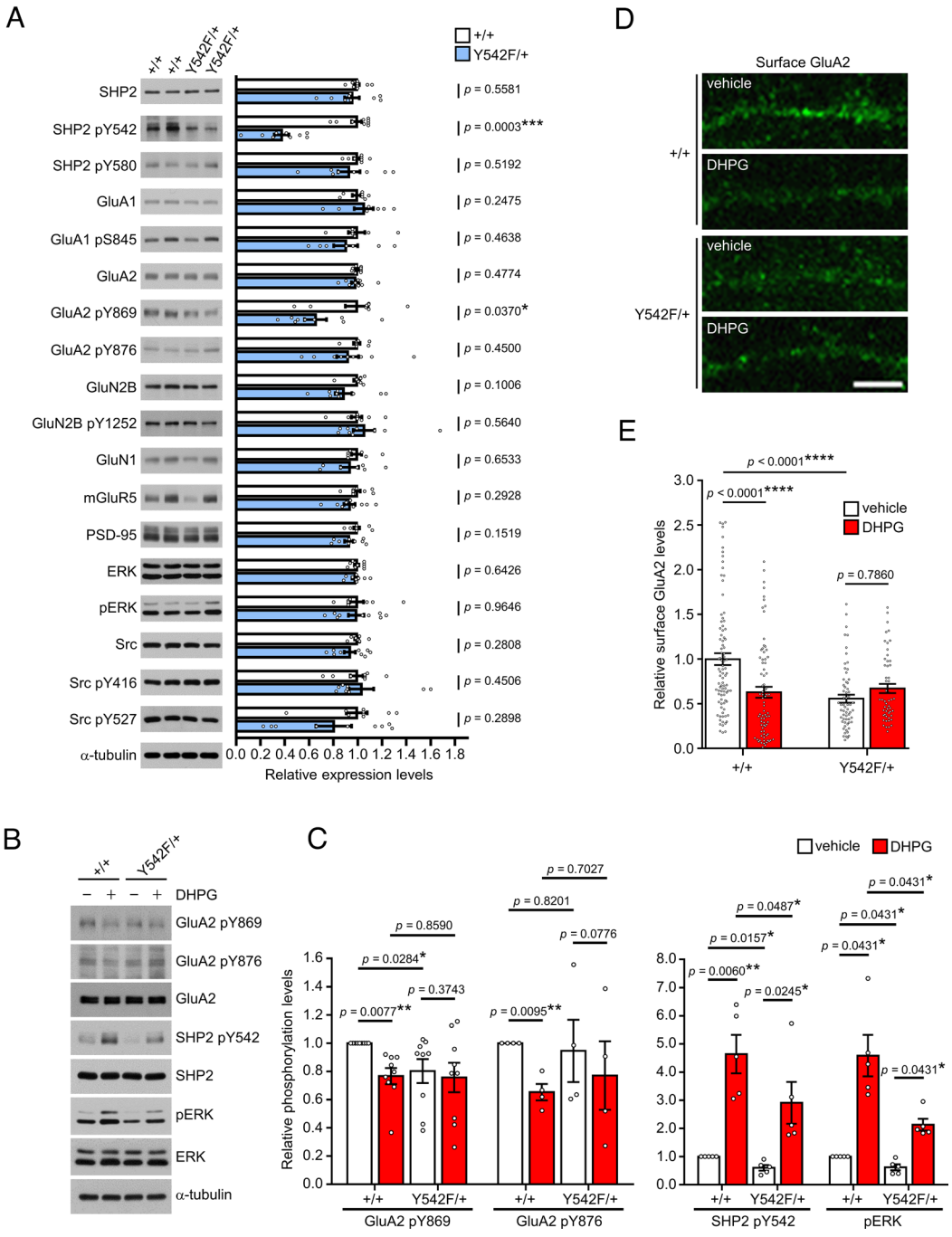

Fig. 5. GluA2 tyrosine phosphorylation and endocytosis are dysregulated in *Ptpn11*$^{Y542F/+}$ mice. (*A*) Crude synaptosomal P2 fractions were prepared from the hippocampi of 5- to 8-wk-old *Ptpn11*$^{Y542F/+}$ mice (Y542F/+) or their WT littermates (+/+). Representative western blots and quantification data are presented (n = 4, number of mice = 7 to 9, unpaired Student's *t* test for SHP2, SHP2 pY580, GluA1 pS845, GluA2 pY876, mGluR5, PSD-95, ERK, Src, and Src pY527; Mann–Whitney *U* test for SHP2 pY542, GluA1, GluA2, GluA2 pY869, GluN2B, GluN2B pY1252, GluN1, pERK, and Src pY416). (*B*) Western blot analysis using primary cultured neurons. (*C*) Quantification data from panel (*B*) (n = 5 to 9, paired Student's *t* test for GluA2 pY876 and SHP2 pY542; Wilcoxon signed-rank test for GluA2 pY869 and pERK). (*D*) After treating primary cultured neurons with 100 μM DHPG for 10 min, neurons were incubated in conditioned medium for 15 min. The surface-expressed GluA2 was visualized using a GluA2 N-terminal antibody under nonpermeabilized conditions. (Scale bar, 7 μm.) (*E*) Quantification of surface-expressed GluA2 from 30-μm-long secondary branches (n = 3, number of branches = 53 to 90, Kruskal–Wallis test with Dunn's multiple comparison test).

and complete PTP activity. Unlike these substrates, in the case of GluA2, SHP2 protects and stabilizes the phosphorylation of GluA2 Y869 after the N-SH2 domain of SHP2 directly binds to it. This indicates that the SH2 fragment of SHP2 is active, whereas the PTP domain is restricted to a closed conformation. Upon SHP2 phosphorylation at Y542 by mGluR5 stimulation, the N-SH2 domain binds to the phospho-Y542 residue, exposing the PTP domain through transition to an open state.

Our study revealed that the phosphorylation status of GluA2 Y869, driven by SHP2, directly correlated with the surface expression of GluA2, both under steady-state conditions and upon mGluR5 stimulation. Notably, while SHP099 treatment reduced surface expression of GluA2 without affecting steady-state GluA2 Y876 phosphorylation, the nonphosphorylatable GluA2 Y876F mutant exhibited increased internalization compared to the WT, under basal conditions. This raises the possibility that SHP2, in

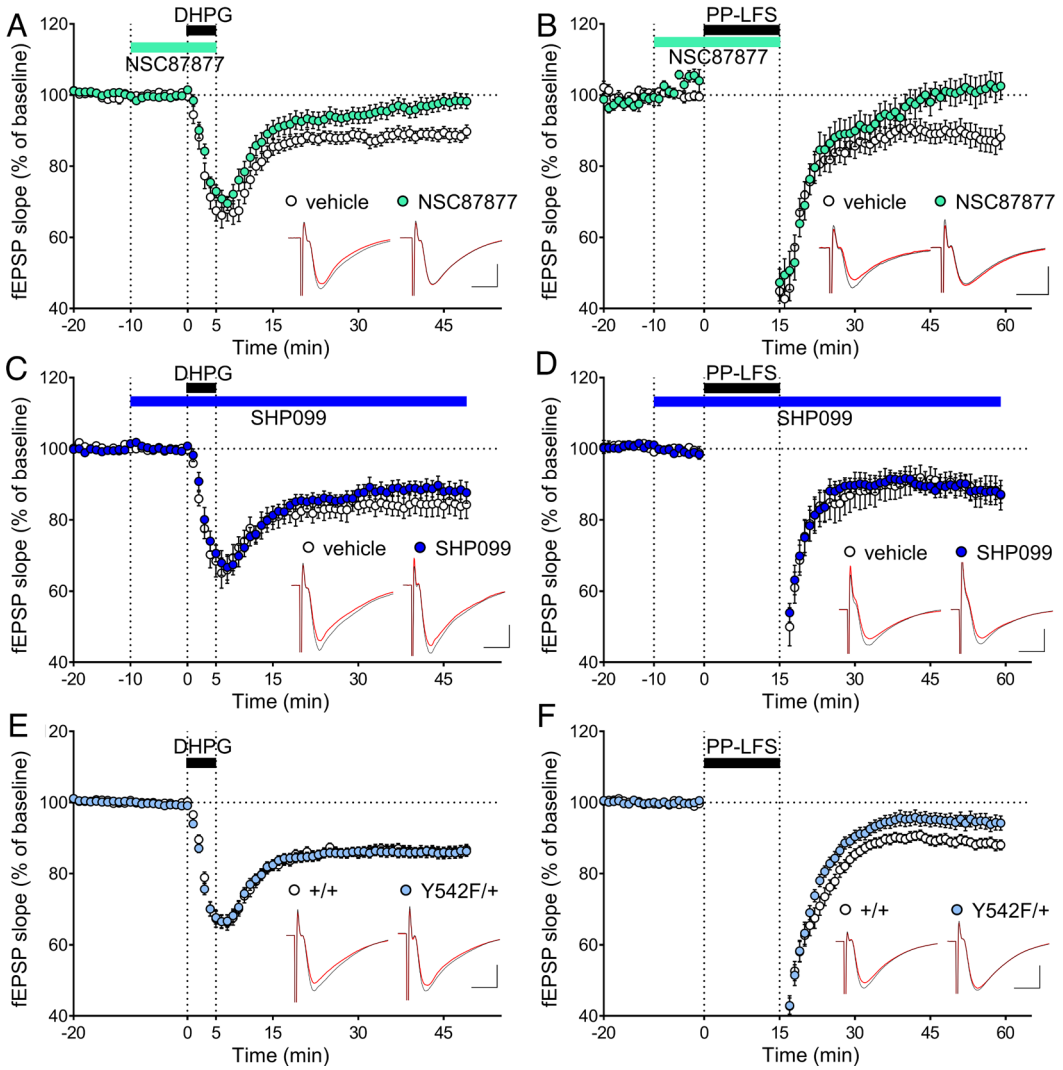

Fig. 6. mGluR-LTD is impaired by SHP2 dysfunction. (*A*–*D*) Effects of pharmacological inhibition of SHP2 on mGluR-LTD. Time course plot of fEPSP slopes of 100 μM DHPG-LTD (*A*) or PP-LFS-LTD (*B*) with or without 10 μM NSC87877 treatment. Time course plot of fEPSP slopes of DHPG-LTD (*C*) or PP-LFS-LTD (*D*) with or without 10 μM SHP099 treatment. For SHP099 experiments, SHP099 was continuously added to the artificial cerebrospinal fluid (ACSF) because of its reversible inhibitory properties. (*E* and *F*) mGluR-LTD in *Ptpn11*$^{Y542F/+}$ mice. Time course plot of fEPSP slopes of DHPG-LTD (*E*) or PP-LFS-LTD (*F*). Sample traces show representative fEPSPs 1 min before (black) and 44 min after (red) induction. (Scale bar, 0.5 mV, 5 ms.) Quantification of the average fEPSP slopes and the number of slices are presented in *SI Appendix*, Fig. S14.

addition to its role in regulating GluA2 phosphorylation, may also function as a scaffold to anchor GluA2 to the neuronal surface. Likewise, recent reports have highlighted the importance of the structural function rather than the enzymatic function of CaMKII and SynGAP in LTP induction (54, 55).

Our in vitro phosphatase assay data showed that SHP2 could dephosphorylate both the GluA2 Y869 and Y876 residues. Kinetic analysis of SHP2 activity on GluA2 revealed that Y869 is a more favorable substrate than Y876. Importantly, we found that Src-induced Y869 phosphorylation is a prerequisite for the complete phosphorylation of Y876, indicating that GluA2 phosphorylation of Y876 can be regulated by the Y869 phosphorylation status. Moreover, in neurons treated with SHP099, Y876 was dephosphorylated by DHPG, even in the absence of SHP2 catalytic activity. This observation could be attributed to the involvement of phosphatases other than SHP2 or may be explained by an indirect effect of Y869 dephosphorylation.

Two Pharmacological Inhibitors of SHP2 with Distinct Mechanisms of Action. Based on our findings using two SHP2 inhibitors with distinct mechanisms of action, we propose the following speculative model for GluA2 regulation by SHP2. Similar to WT SHP2, SHP2 treated with NSC87877 maintained its ability to undergo a closed-to-open, conformational transition, but lost its catalytic activity (51). Consequently, NSC87877-treated SHP2 retains its PTP-independent function, which subsequently contributes to the maintenance of steady-state GluA2 tyrosine phosphorylation and surface expression. However, upon DHPG stimulation, it is unable to dephosphorylate GluA2 tyrosine residues, despite transitioning to an open conformation, resulting in impaired GluA2 internalization and mGluR-LTD. In contrast, the closed conformation of SHP2 induced by SHP099 adopts a rigid, inflexible structure that is resistant to the transition from the closed to the open conformation, both under steady-state conditions and mGluR5 stimulation. Because SHP099 inhibits not only the scaffolding but also the PTP activity of SHP2, it is likely that SHP2's function on GluA2 Y869 is mainly protective and that dephosphorylation is driven by PTPs other than SHP2 in the basal state.

We observed that the two different SHP2 inhibitors had distinct effects on the tyrosine phosphorylation levels of GluA2 both in the basal and DHPG-stimulated conditions. Although other PTPs may be involved in the tyrosine dephosphorylation

of GluA2, our data suggest that SHP2 is the main PTP that dephosphorylates GluA2 phospho-Y869 and phospho-Y876 during mGluR stimulation (Fig. 4 *A* and *B*). For the Y869 residue, as DHPG treatment did not lead to additional reduction of the phospho-Y869 level in the presence of SHP099, it is unlikely that activation of other PTPs is responsible for DHPG-induced Y869 dephosphorylation. Moreover, after cotreatment with NSC87877 and DHPG, phospho-Y869 levels remained consistent, implying that the catalytic activity of SHP2 rather than the loss of its protective function reduces the phospho-Y869 level when treated with DHPG alone (Fig. 4 *A* and *B*). Considering that SHP2 can directly dephosphorylate phospho-Y869 in vitro (Fig. 3 *D* and *E*), phospho-Y869 appears to be directly dephosphorylated by SHP2 upon mGluR stimulation. Regarding the Y876 residue, unlike the Y869 residue, neither NSC87877 nor SHP099 treatment alone altered phospho-Y876 levels, indicating that SHP2 has minimal protective activity against the Y876 residue in the basal state (Fig. 4 *A* and *B*). This difference may arise from the fact that SHP2 directly interacts with Y869-phosphorylated GluA2 but not with Y876-phosphorylated GluA2 (Fig. 3*B*). However, upon stimulation by DHPG, the protective function for the Y876 residue appears to be reinstated through an exposed N-SH2 stretch as the catalytic activity of SHP2 increases. In the presence of NSC87877, the protective function of SHP2 prevents other PTPs from dephosphorylating phospho-Y876 while SHP2's own catalytic activity is blocked by NSC87877, resulting in an unchanged phospho-Y876 level. In contrast, in the presence of SHP099, both the protective function and catalytic activity of SHP2 were blocked, allowing other PTPs to dephosphorylate phospho-Y876 (Fig. 4 *A* and *B*). Because the PTP of SHP2 also directly dephosphorylates phospho-Y876 in vitro (Fig. 3 *D* and *E*), it is likely that upon mGluR stimulation, phospho-Y876 can be dephosphorylated by both SHP2 and other PTPs depending on the molecular context.

Given that changes in Y869-phosphorylated GluA2 primarily represent extrasynaptic events (*SI Appendix*, Fig. S9), the decrease in SHP2 scaffolding after SHP099 treatment may contribute less to basal synaptic transmission and strength, as shown in the unchanged baseline fEPSP during SHP099 treatment (Fig. 6 *C* and *D*). Then, the preferential extrasynaptic distribution of phospho-Y869 raises a question as to how the phosphorylation of extrasynaptic AMPA receptors influences the removal of synaptic AMPA receptors. The precise mechanism remains elusive; however, considering that mGluR-LTD is normal with SHP099, which maintains Y869 in a dephosphorylated state, whereas it is impaired with NSC87877, which blocks dephosphorylation of both residues, GluA2 Y876 may be a primary determinant in LTD expression, with dephosphorylated Y869 acting as a permissive requirement. Further investigation on the differential role of the two tyrosine residues in mGluR-LTD is needed.

Moreover, we observed that SHP099 treatment reduced the interaction of SHP2 with GluA2, effectively depriving the PTP-independent function of SHP2 in regulating GluA2 tyrosine phosphorylation, as if SHP2 were absent. In addition, the capacity of SHP2 to anchor GluA2 to the neuronal surface may also contribute to the decline in basal GluA2 surface expression in SHP099-treated neurons. The SHP099-induced reduction in basal surface GluA2 expression may allow mGluR-stimulated neurons to adopt an alternative GluA2-independent mechanism of LTD, resulting in the manifestation of normal mGluR-LTD. This notion is supported by previous findings demonstrating that the young GluA2 knock-out (KO) mice exhibit intact mGluR-LTD despite the absence of surface-expressed GluA2 (56–58). Therefore, in addition to the importance of the different conformational states of SHP2, the structural flexibility that allows SHP2 to transition from the closed-to-open conformations appears to be an important factor influencing its function (59). It is necessary to delineate the precise conformational changes in SHP2, induced by mGluR5 stimulation.

SHP2 Is Involved in Multiple Forms of Synaptic Plasticity. We found that pharmacological inhibition of SHP2 catalytic activity impaired mGluR-LTD in hippocampal SC-CA1 synapses (Fig. 6 *A* and *B* and *SI Appendix*, Fig. S14*A*). SHP2 is known to be involved in multiple forms of synaptic plasticity, including LTP, via the regulation of AMPA receptor trafficking. For instance, chemical LTP stimulation or tetrodotoxin (TTX)-induced synaptic upscaling increases SHP2 Y542 phosphorylation and surface GluA1 expression in the hippocampus (45, 46), whereas chemical LTD stimulation reduces SHP2 Y542 phosphorylation and surface GluA1 expression (60). Consistently, NSC87877 blocks LTP by suppressing the GluA1 phosphorylation and membrane trafficking (45). Expression of SHP2 D61G, a GOF mutation, enhances AMPA receptor-mediated current and increases the number of synaptic AMPA receptors by enhancing Ras-ERK signaling in the adult mouse hippocampus (39). Additionally, SHP2 D61G prevents bicuculline-induced synaptic downscaling by increasing its association with PSD-95 (61). TTX-mediated synaptic upscaling is impaired in neurons expressing catalytically inactive C459S SHP2 or in SHP2 KO neurons (46). These reports show that SHP2 is critically involved in the modulation of LTP and homeostatic plasticity.

In juvenile *Ptpn11*$^{D61G/+}$ mice, hyperactive SHP2 impairs NMDAR function by directly dephosphorylating GluN2B Y1252 and disrupting Nck2 scaffold binding (40). In contrast, phosphorylation levels of GluN2B Y1472 and GluN2A Y1325 were increased in the hippocampus of mice lacking SHP2 (44).

We demonstrated that the catalytic activity of SHP2 is required for mGluR-LTD. In contrast, Kusakari et al. (38) reported that DHPG-induced mGluR-LTD was intact in SHP2 conditional KO mice lacking SHP2 in postnatal CaMKII-positive neurons. Although the reason for this discrepancy is unclear, SHP2 KO neurons may have a similar phenotype to SHP099-treated neurons. In both cases, the absence of surface GluA2 can potentially activate an alternative GluA2-independent mechanism for mGluR-LTD (56–58). We observed only partial impairment of mGluR-LTD in *Ptpn11*$^{Y542F/+}$ mice, whereas mGluR-LTD was fully blocked by NSC87877 treatment. Our results indicate that SHP2 is involved in mGluR-LTD; however, the precise mechanism by which SHP2 modulates bidirectional synaptic changes remains unclear.

Does SHP2 Bridge the mGluR and RAS Pathways? *PTPN11* mutations in humans are associated with RASopathies, a group of disorders commonly characterized by neurodevelopmental defects. Studies of RASopathy-related mutations have shown hyperactivation of the Ras-ERK pathway, learning and behavioral deficits, and structural abnormalities in the brain (62). Dysregulation of group I mGluR signaling in the mammalian target of rapamycin (mTOR) and MAPK/ERK pathways for protein translation has been implicated in the pathogenesis of neurodevelopmental disorders, including autism spectrum disorders (ASDs), fragile X syndrome (FXS), and intellectual disability (9, 63, 64). The use of mGluR5 antagonists to suppress exaggerated mGluR signaling has been proposed as a potential therapy for ASD (63). Since SHP2 has also been shown to regulate the mTOR pathway (64), SHP2 may

function as a shared downstream effector of mGluR5 in the mTOR and Ras-ERK pathways (37). Therefore, we propose a model in which SHP2 underlies the convergent synaptic pathophysiology of ASD and RASopathies, highlighting SHP2 as a promising therapeutic target for these disorders.

Materials and Methods

Antibodies and Reagents. Anti-GluA2 pY869 antibody was prepared by cross-adsorbing a commercially available anti-GluA2 p3Y antibody (Cell Signaling Technology, 3921) with GST-GluA2ct Y869F phosphorylated with Src kinase. Briefly, GST-GluA2ct Y869F was phosphorylated using lysate from HEK 293 T cells overexpressing Src in a kinase assay buffer (25 mM HEPES, pH 7.5, 10 mM $MgCl_2$, 5 mM $MnCl_2$, 2 mM DTT, and 5 mM ATP) for 2 h at 30 °C. The beads were washed and incubated with anti-GluA2 p3Y antibody for 48 h at 4 °C, and the resulting supernatant was collected. Additional comprehensive details of materials and methods are provided in *SI Appendix, Materials and Methods*.

Data, Materials, and Software Availability. All study data are included in the article and/or *SI Appendix*.

ACKNOWLEDGMENTS. This work was supported by grants from the National Research Foundation (NRF) of Korea (NRF-2018R1A2B6004759, NRF-2020R1A5A1019023, and NRF-2022R1A2C1004913 to Y.H.S.; NRF-2023R1A2C2003229 and NRF-2018R1A5A2025964 to Y.-S.L.) and the Korea Dementia Research Project through the Korea Dementia Research Center (KDRC) (HU21C0071 to Y.H.S.).

Author affiliations: [a]Department of Biomedical Sciences, Seoul National University College of Medicine, Seoul 03080, South Korea; [b]Neuroscience Research Institute, Medical Research Center, Seoul National University College of Medicine, Seoul 03080, South Korea; [c]Transplantation Research Institute, Medical Research Center, Seoul National University College of Medicine, Seoul 03080, South Korea; and [d]Department of Physiology, Seoul National University College of Medicine, Seoul 03080, South Korea

Author contributions: Sanghyeon Lee and Y.H.S. designed research; Sanghyeon Lee, J.K., H.-H.R., H.J., D.L., Seungha Lee, and J.-m.S. performed research; Sanghyeon Lee, J.K., H.-H.R., H.J., Y.-S.L., and Y.H.S. analyzed data; and Y.H.S. wrote the paper.

1. G. H. Diering, R. L. Huganir, The AMPA receptor code of synaptic plasticity. *Neuron* **100**, 314–329 (2018).
2. R. C. Malenka, M. F. Bear, LTP and LTD: An embarrassment of riches. *Neuron* **44**, 5–21 (2004).
3. S. M. Dudek, M. F. Bear, Homosynaptic long-term depression in area CA1 of hippocampus and effects of N-methyl-D-aspartate receptor blockade. *Proc. Natl. Acad. Sci. U.S.A.* **89**, 4363–4367 (1992).
4. R. M. Mulkey, R. C. Malenka, Mechanisms underlying induction of homosynaptic long-term depression in area CA1 of the hippocampus. *Neuron* **9**, 967–975 (1992).
5. Z. I. Bashir, D. E. Jane, D. C. Sunter, J. C. Watkins, G. L. Collingridge, Metabotropic glutamate receptors contribute to the induction of long-term depression in the CA1 region of the hippocampus. *Eur. J. Pharmacol.* **239**, 265–266 (1993).
6. P. K. Stanton, S. Chattarji, T. J. Sejnowski, 2-Amino-3-phosphonopropionic acid, an inhibitor of glutamate-stimulated phosphoinositide turnover, blocks induction of homosynaptic long-term depression, but not potentiation, in rat hippocampus. *Neurosci. Lett.* **127**, 61–66 (1991).
7. G. L. Collingridge, S. Peineau, J. G. Howland, Y. T. Wang, Long-term depression in the CNS. *Nat. Rev. Neurosci.* **11**, 459–473 (2010).
8. R. L. Huganir, R. A. Nicoll, AMPARs and synaptic plasticity: The last 25 years. *Neuron* **80**, 704–717 (2013).
9. C. Luscher, K. M. Huber, Group 1 mGluR-dependent synaptic long-term depression: Mechanisms and implications for circuitry and disease. *Neuron* **65**, 445–459 (2010).
10. E. M. Snyder *et al.*, Internalization of ionotropic glutamate receptors in response to mGluR activation. *Nat. Neurosci.* **4**, 1079–1085 (2001).
11. T. Hayashi, R. L. Huganir, Tyrosine phosphorylation and regulation of the AMPA receptor by SRC family tyrosine kinases. *J. Neurosci. Offi. J. Soc. Neurosci.* **24**, 6152–6160 (2004).
12. R. Scholz *et al.*, AMPA receptor signaling through BRAG2 and Arf6 critical for long-term synaptic depression. *Neuron* **66**, 768–780 (2010).
13. T. Hayashi, H. Umemori, M. Mishina, T. Yamamoto, The AMPA receptor interacts with and signals through the protein tyrosine kinase Lyn. *Nature* **397**, 72–76 (1999).
14. K. Kohda *et al.*, The delta2 glutamate receptor gates long-term depression by coordinating interactions between two AMPA receptor phosphorylation sites. *Proc. Natl. Acad. Sci. U.S.A.* **110**, E948–E957 (2013).
15. Y. Zhang *et al.*, The tyrosine phosphatase STEP mediates AMPA receptor endocytosis after metabotropic glutamate receptor stimulation. *J. Neurosci. Offi. J. Soci. Neurosci.* **28**, 10561–10566 (2008).
16. C. M. Gladding *et al.*, Tyrosine dephosphorylation regulates AMPAR internalisation in mGluR-LTD. *Mol. Cell Neurosci.* **40**, 267–279 (2009).
17. C. C. Huang, K. S. Hsu, Sustained activation of metabotropic glutamate receptor 5 and protein tyrosine phosphatases mediate the expression of (S)-3,5-dihydroxyphenylglycine-induced long-term depression in the hippocampal CA1 region. *J. Neurochem.* **96**, 179–194 (2006).
18. P. R. Moult, S. A. Correa, G. L. Collingridge, S. M. Fitzjohn, Z. I. Bashir, Co-activation of p38 mitogen-activated protein kinase and protein tyrosine phosphatase underlies metabotropic glutamate receptor-dependent long-term depression. *J. Physiol.* **586**, 2499–2510 (2008).
19. P. R. Moult *et al.*, Tyrosine phosphatases regulate AMPA receptor trafficking during metabotropic glutamate receptor-mediated long-term depression. *J. Neurosci. Offi. J. Soc. Neurosci.* **26**, 2544–2554 (2006).
20. P. R. Moult, R. Schnabel, I. C. Kilpatrick, Z. I. Bashir, G. L. Collingridge, Tyrosine dephosphorylation underlies DHPG-induced LTD. *Neuropharmacology* **43**, 175–180 (2002).
21. N. Kemp, Z. I. Bashir, NMDA receptor-dependent and -independent long-term depression in the CA1 region of the adult rat hippocampus in vitro. *Neuropharmacology* **36**, 397–399 (1997).
22. N. Kemp, Z. I. Bashir, Induction of LTD in the adult hippocampus by the synaptic activation of AMPA/kainate and metabotropic glutamate receptors. *Neuropharmacology* **38**, 495–504 (1999).
23. S. M. Fitzjohn, A. E. Kingston, D. Lodge, G. L. Collingridge, DHPG-induced LTD in area CA1 of juvenile rat hippocampus; characterisation and sensitivity to novel mGlu receptor antagonists. *Neuropharmacology* **38**, 1577–1583 (1999).
24. M. J. Palmer, A. J. Irving, G. R. Seabrook, D. E. Jane, G. L. Collingridge, The group I mGlu receptor agonist DHPG induces a novel form of LTD in the CA1 region of the hippocampus. *Neuropharmacology* **36**, 1517–1532 (1997).
25. G. Ahmadian *et al.*, Tyrosine phosphorylation of GluR2 is required for insulin-stimulated AMPA receptor endocytosis and LTD. *EMBO J.* **23**, 1040–1050 (2004).
26. C. J. Fox, K. Russell, A. K. Titterness, Y. T. Wang, B. R. Christie, Tyrosine phosphorylation of the GluR2 subunit is required for long-term depression of synaptic efficacy in young animals in vivo. *Hippocampus* **17**, 600–605 (2007).
27. M. Fukaya *et al.*, BRAG2a mediates mGluR-dependent AMPA receptor internalization at excitatory postsynapses through the interaction with PSD-95 and endophilin 3. *J. Neurosci. Offi. J. Soc. Neurosci.* **40**, 4277–4296 (2020).
28. S. M. Goebel-Goody *et al.*, Therapeutic implications for striatal-enriched protein tyrosine phosphatase (STEP) in neuropsychiatric disorders. *Pharmacol. Rev.* **64**, 65–87 (2012).
29. A. J. H. Yong *et al.*, Tyrosine phosphorylation of the AMPA receptor subunit GluA2 gates homeostatic synaptic plasticity. *Proc. Natl. Acad. Sci. U.S.A.* **117**, 4948–4958 (2020).
30. M. Tajan, A. de Rocca Serra, P. Valet, T. Edouard, A. Yart, SHP2 sails from physiology to pathology. *Eur. J. Med. Genet.* **58**, 509–525 (2015).
31. M. Dance, A. Montagner, J. P. Salles, A. Yart, P. Raynal, The molecular functions of Shp2 in the Ras/Mitogen-activated protein kinase (ERK1/2) pathway. *Cell Signal.* **20**, 453–459 (2008).
32. B. G. Neel, H. Gu, L. Pao, The 'Shp'ing news: SH2 domain-containing tyrosine phosphatases in cell signaling. *Trends Biochem. Sci.* **28**, 284–293 (2003).
33. P. Hof, S. Pluskey, S. Dhe-Paganon, M. J. Eck, S. E. Shoelson, Crystal structure of the tyrosine phosphatase SHP-2. *Cell* **92**, 441–450 (1998).
34. Y. Tao *et al.*, A novel partially open state of SHP2 points to a "multiple gear" regulation mechanism. *J. Biol. Chem.* **296**, 100538 (2021).
35. Y. N. Chen *et al.*, Allosteric inhibition of SHP2 phosphatase inhibits cancers driven by receptor tyrosine kinases. *Nature* **535**, 148–152 (2016).
36. V. Vemulapalli *et al.*, Time-resolved phosphoproteomics reveals scaffolding and catalysis-responsive patterns of SHP2-dependent signaling. *Elife* **10**, e64251 (2021).
37. H.-H. Ryu, S. Y. Kim, Y.-S. Lee, Connecting the dots between SHP2 and glutamate receptors. *Korean J. Physiol. Pharmacol.* **24**, 129–135 (2020).
38. S. Kusakari *et al.*, Shp2 in forebrain neurons regulates synaptic plasticity, locomotion, and memory formation in mice. *Mol. Cell Biol.* **35**, 1557–1572 (2015).
39. Y. S. Lee *et al.*, Mechanism and treatment for learning and memory deficits in mouse models of Noonan syndrome. *Nat. Neurosci.* **17**, 1736–1743 (2014).
40. A. D. Levy *et al.*, Noonan syndrome-associated SHP2 dephosphorylates GluN2B to regulate NMDA receptor function. *Cell Rep.* **24**, 1523–1535 (2018).
41. S. Y. Lin *et al.*, Brain-derived neurotrophic factor enhances association of protein tyrosine phosphatase PTP1D with the NMDA receptor subunit NR2B in the cortical postsynaptic density. *Brain Res. Mol. Brain Res.* **70**, 18–25 (1999).
42. J. Y. Oh, S. Rhee, A. J. Silva, Y. S. Lee, H. K. Kim, Noonan syndrome-associated SHP2 mutation differentially modulates the expression of postsynaptic receptors according to developmental maturation. *Neurosci. Lett.* **649**, 41–47 (2017).
43. H. Y. Peng, G. D. Chen, C. Y. Lai, M. C. Hsieh, T. B. Lin, Spinal SIRPalpha1–SHP2 interaction regulates spinal nerve ligation–induced neuropathic pain via PSD-95–dependent NR2B activation in rats. *Pain* **153**, 1042–1053 (2012).
44. X. Yan *et al.*, Increased Src family kinase activity disrupts excitatory synaptic transmission and impairs remote fear memory in forebrain Shp2-deficient mice. *Mol. Neurobiol.* **54**, 7235–7250 (2017).
45. B. Zhang *et al.*, Increased activity of Src homology 2 domain containing phosphotyrosine phosphatase 2 (Shp2) regulates activity-dependent AMPA receptor trafficking. *J. Biol. Chem.* **291**, 18856–18866 (2016).
46. B. Zhang, W. Lu, Src homology 2 domain-containing phosphotyrosine phosphatase 2 (Shp2) controls surface GluA1 protein in synaptic homeostasis. *J. Biol. Chem.* **292**, 15481–15488 (2017).
47. A. M. Bennett, T. L. Tang, S. Sugimoto, C. T. Walsh, B. G. Neel, Protein-tyrosine-phosphatase SHPTP2 couples platelet-derived growth factor receptor beta to Ras. *Proc. Natl. Acad. Sci. U.S.A.* **91**, 7335–7339 (1994).
48. W. Lu, D. Gong, D. Bar-Sagi, P. A. Cole, Site-specific incorporation of a phosphotyrosine mimetic reveals a role for tyrosine phosphorylation of SHP-2 in cell signaling. *Mol. Cell* **8**, 759–769 (2001).
49. J. Yang *et al.*, Crystal structure of human protein-tyrosine phosphatase SHP-1. *J. Biol. Chem.* **278**, 6516–6520 (2003).
50. D. Jingu *et al.*, Protein tyrosine phosphatase Shp2 positively regulates cold stress-induced tyrosine phosphorylation of SIRPα in neurons. *Biochem. Biophys. Res. Commun.* **569**, 72–78 (2021).
51. L. Chen *et al.*, Discovery of a novel shp2 protein tyrosine phosphatase inhibitor. *Mol. Pharmacol.* **70**, 562–570 (2006).
52. H. Ohnishi, Y. Murata, H. Okazawa, T. Matozaki, Src family kinases: Modulators of neurotransmitter receptor function and behavior. *Trends Neurosci.* **34**, 629–637 (2011).
53. B. A. Ballif, G. R. Carey, S. R. Sunyaev, S. P. Gygi, Large-scale identification and evolution indexing of tyrosine phosphorylation sites from murine brain. *J. Proteome Res.* **7**, 311–318 (2008).

54. J. E. Tullis *et al.*, LTP induction by structural rather than enzymatic functions of CaMKII. *Nature* **621**, 146–153 (2023).
55. Y. Araki *et al.*, SynGAP regulates synaptic plasticity and cognition independently of its catalytic activity. *Science* **383**, eadk1291 (2024).
56. Z. Jia *et al.*, Enhanced LTP in mice deficient in the AMPA receptor GluR2. *Neuron* **17**, 945–956 (1996).
57. Y. Meng, Y. Zhang, Z. Jia, Synaptic transmission and plasticity in the absence of AMPA glutamate receptor GluR2 and GluR3. *Neuron* **39**, 163–176 (2003).
58. F. Cao, Z. Zhou, S. Cai, W. Xie, Z. Jia, Hippocampal Long-term depression in the presence of calcium-permeable AMPA receptors. *Front Synaptic Neurosci.* **10**, 41 (2018).
59. G. Zhu *et al.*, Phase separation of disease-associated SHP2 mutants underlies MAPK hyperactivation. *Cell* **183**, 490–502.e418 (2020).
60. H. Zhou *et al.*, The down-regulation of tyrosine phosphatase SHP2 activity is involved in the removal of surface AMPA receptors in long term depression. *Neurosci. Lett.* **779**, 136636 (2022).
61. W. Lu, H. Ai, F. Xue, Y. Luan, B. Zhang, The Noonan syndrome-associated D61G variant of the protein tyrosine phosphatase SHP2 prevents synaptic down-scaling. *J. Biol. Chem.* **295**, 10023–10031 (2020).
62. K. A. Rauen, The RASopathies. *Annu. Rev. Genom. Human Genet.* **14**, 355–369 (2013).
63. M. F. Bear, K. M. Huber, S. T. Warren, The mGluR theory of fragile X mental retardation. *Trends Neurosci.* **27**, 370–377 (2004).
64. S. C. Borrie, H. Brems, E. Legius, C. Bagni, Cognitive dysfunctions in intellectual disabilities: The contributions of the Ras-MAPK and PI3K-AKT-mTOR pathways. *Annu. Rev. Genom. Hum. Genet.* **18**, 115–142 (2017).